

Nanotomy-based production of transferable and dispersible graphene nanostructures of controlled shape and size

Nihar Mohanty¹, David Moore², Zhiping Xu³, T.S. Sreeprasad¹, Ashvin Nagaraja¹, Alfredo Alexander Rodriguez¹ & Vikas Berry¹

¹ Department of Chemical Engineering, Kansas State University, Manhattan, Kansas 66506, USA.

² Microscopy and Analytical Imaging Laboratory, University of Kansas, Lawrence, Kansas 66045, USA.

³ Department of Engineering Mechanics and Center for Nano and Micro Mechanics, Tsinghua University, Beijing 100084, China.



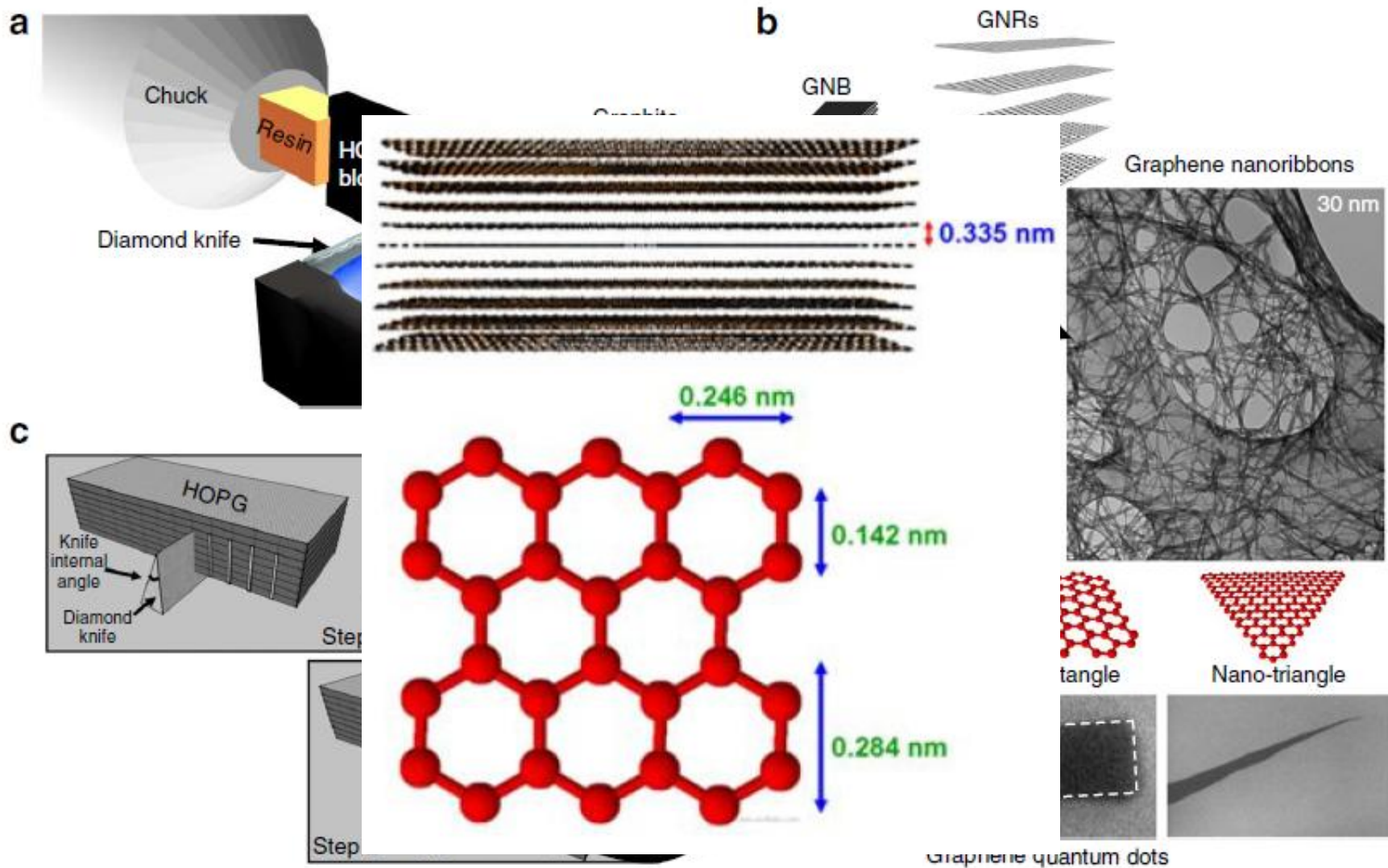
NATURECOMMUNICATIONS | 3:844 | DOI: 10.1038/ncomms1834 | www.nature.com/naturecommunications

Published 15 May 2012

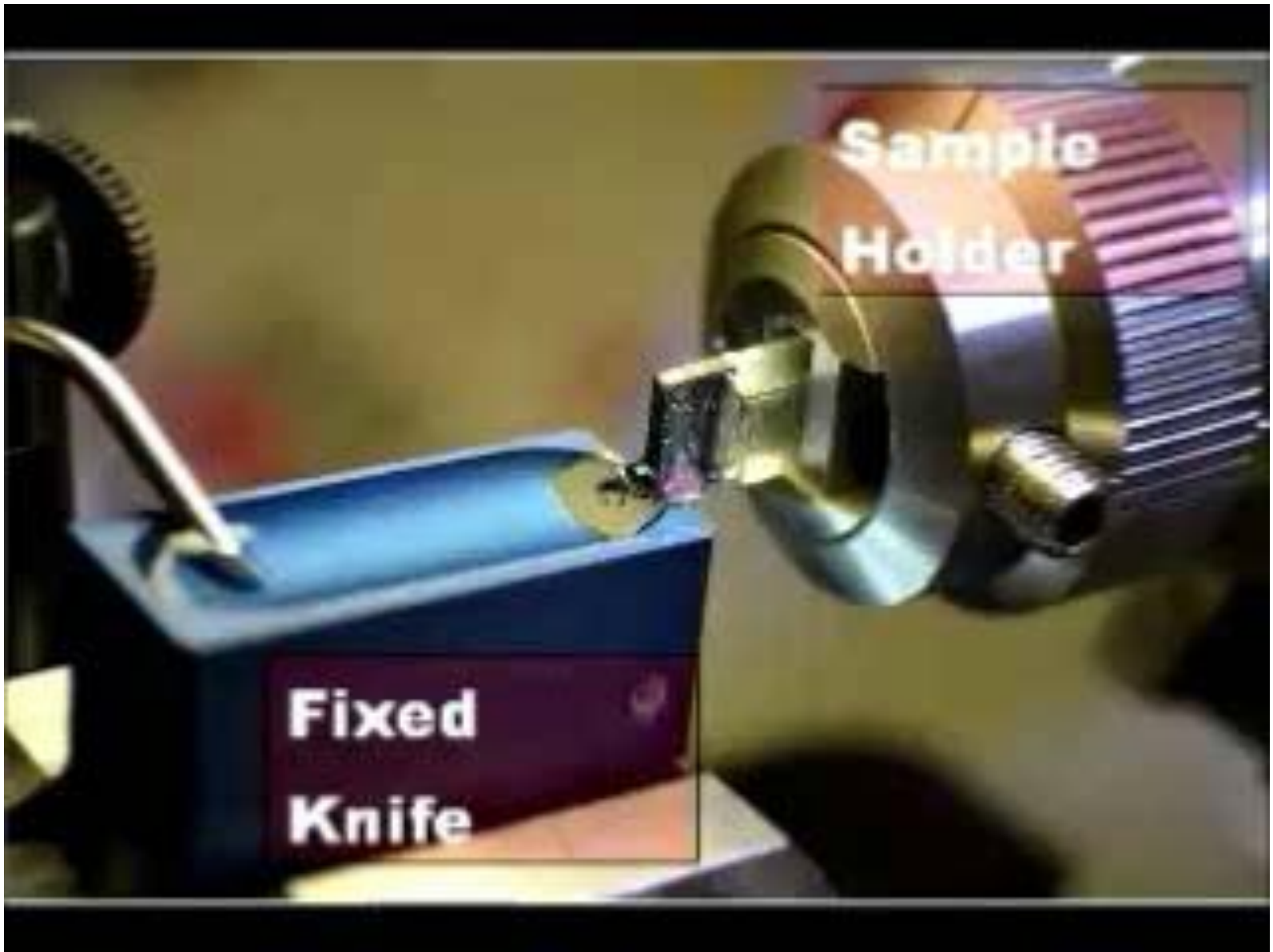
Soujit SenGupta
Date: 01.06.2012

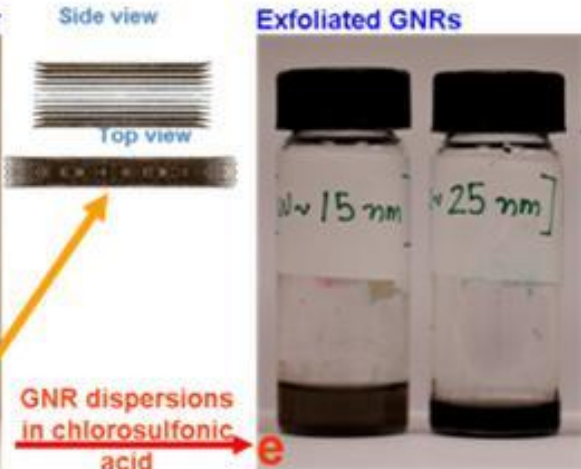
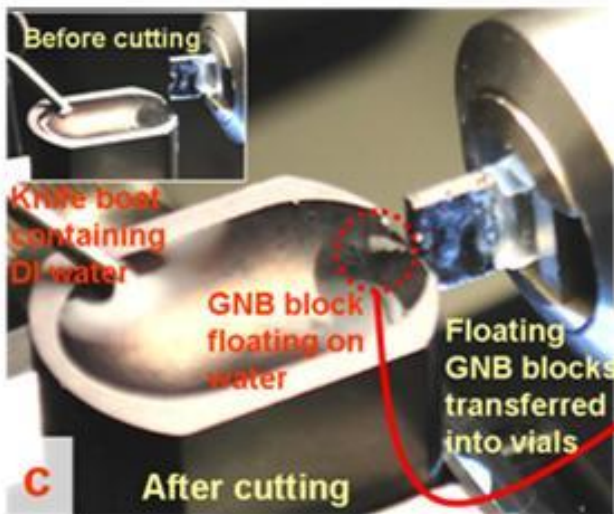
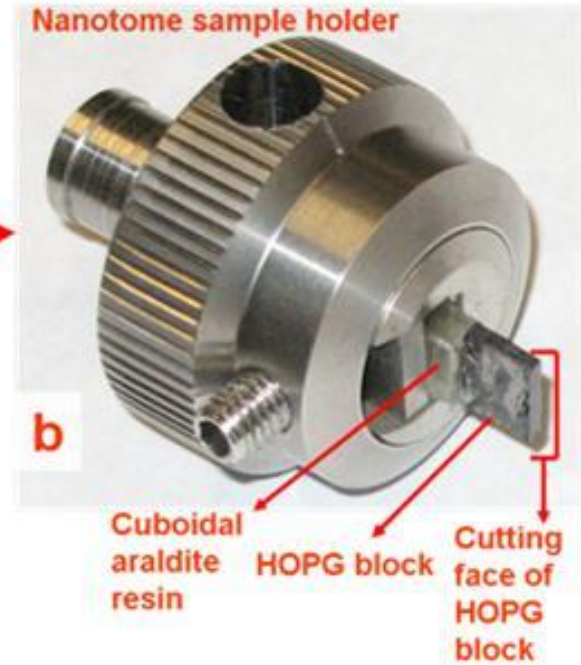
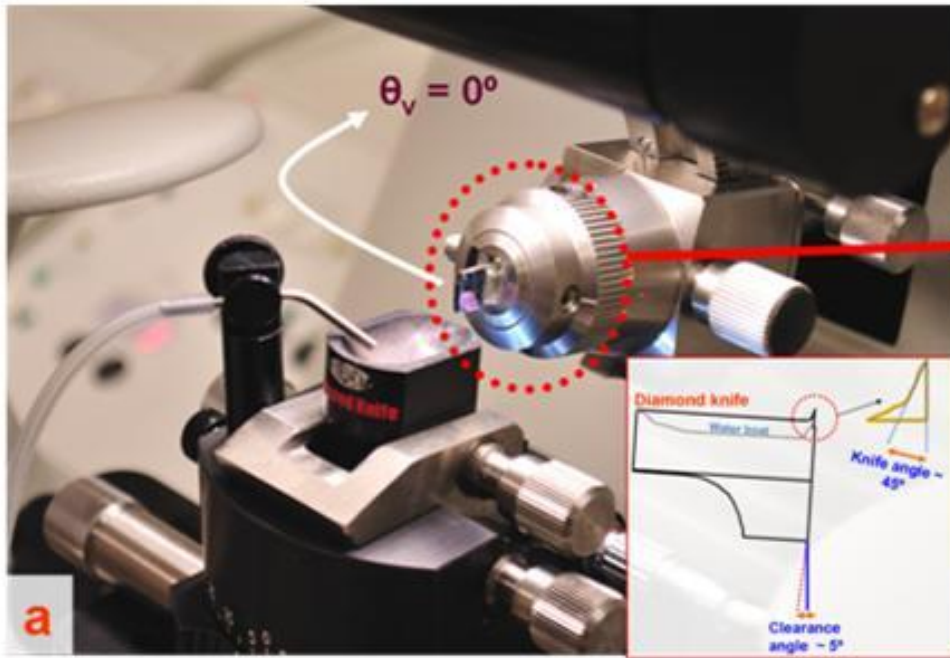
Background

- The shape/size dependent quantum confinement in graphene nanostructures (GNs) control their electrical, magnetic and optical properties.
- There is a need for a process to synthesize GNs with varied, but controlled, shapes and defined size over a wide range such that the GNs can be easily transferred to different substrates or dispersed in different solvents.
- Current top-down techniques to produce GNs include the following:
 - lithography challenging to disperse GNs in solvents or to transfer to other substrates, low edge-smoothness, low throughput.
 - chemical and sono-chemical methods produces uncontrolled size/shape.
 - unzipping of carbon nanotubes (CNTs)—restrictive to graphene nanoribbons, uncontrolled size
 - opening of Fullerenes—produces substrate-bound circular GNs, uncontrolled shape.
- Bottom-up approaches like Diels-Alder reaction fails to produce more than 100 GQDs.

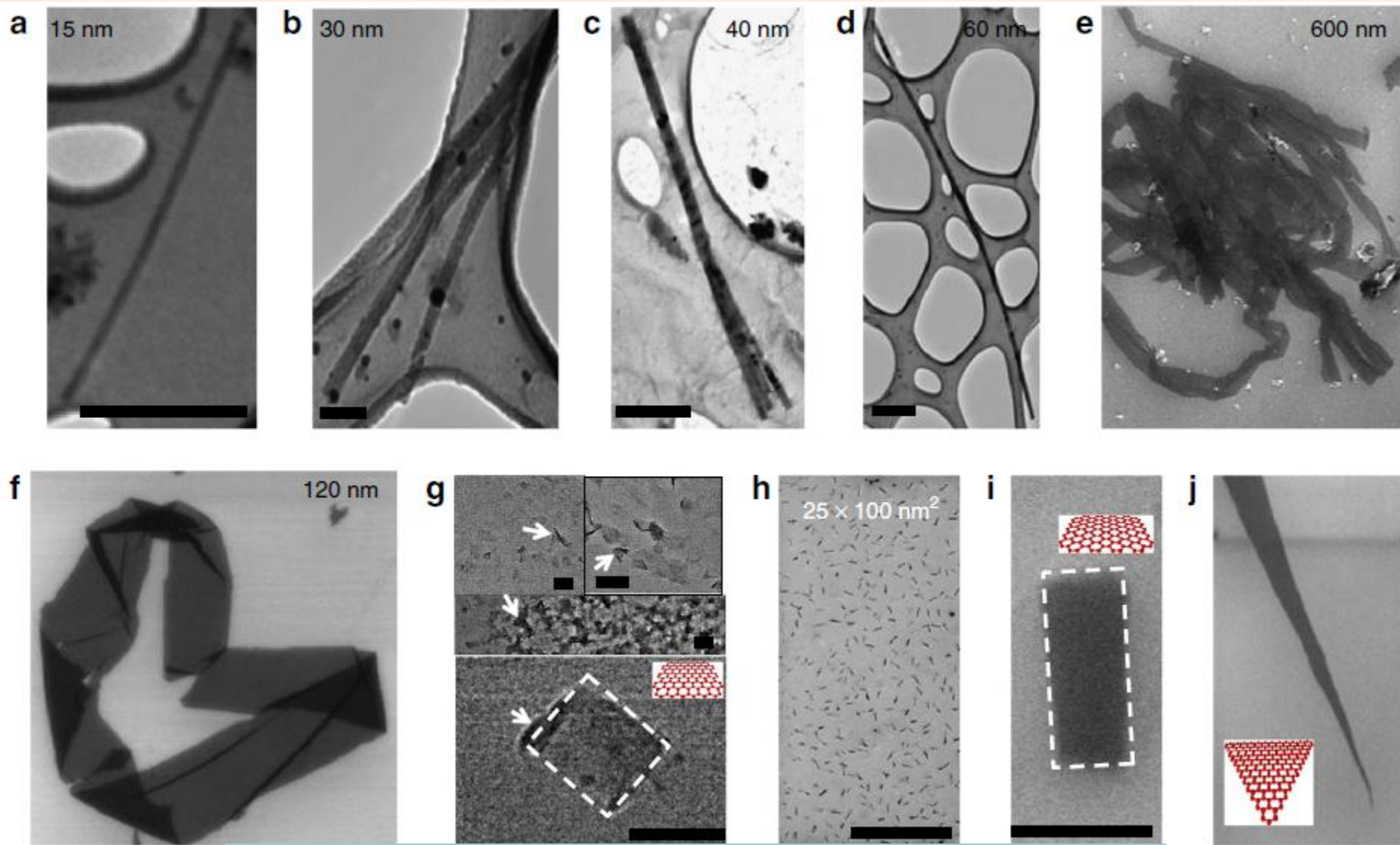


Schematic diagram for the GN production process.

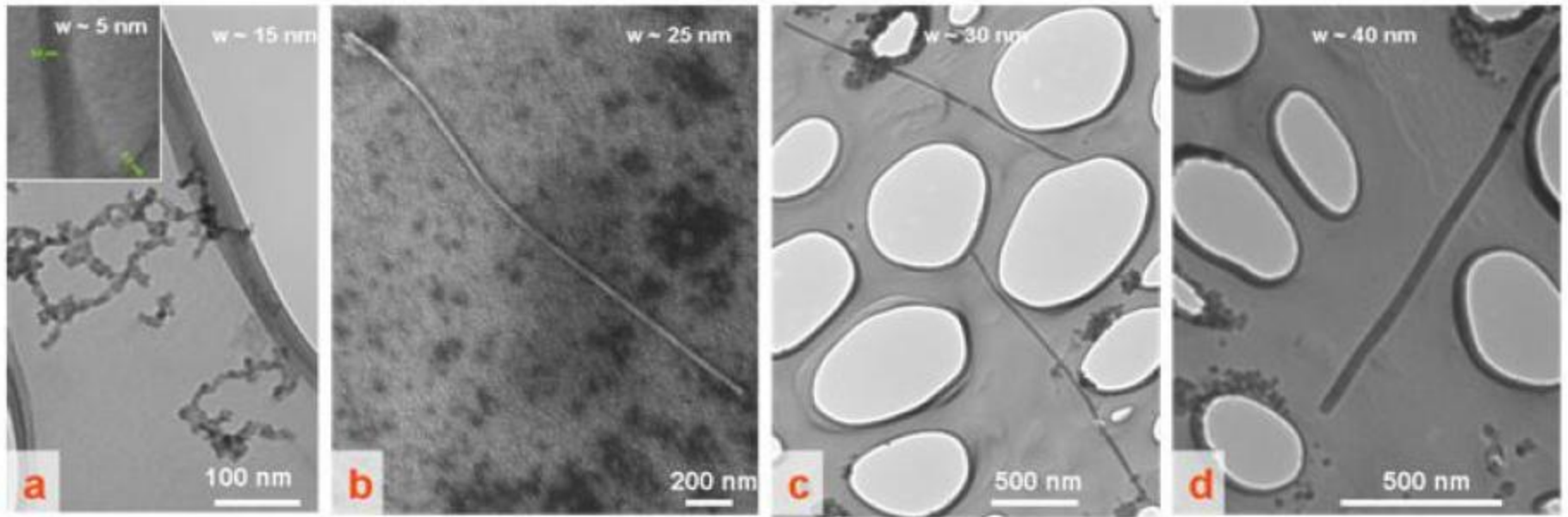




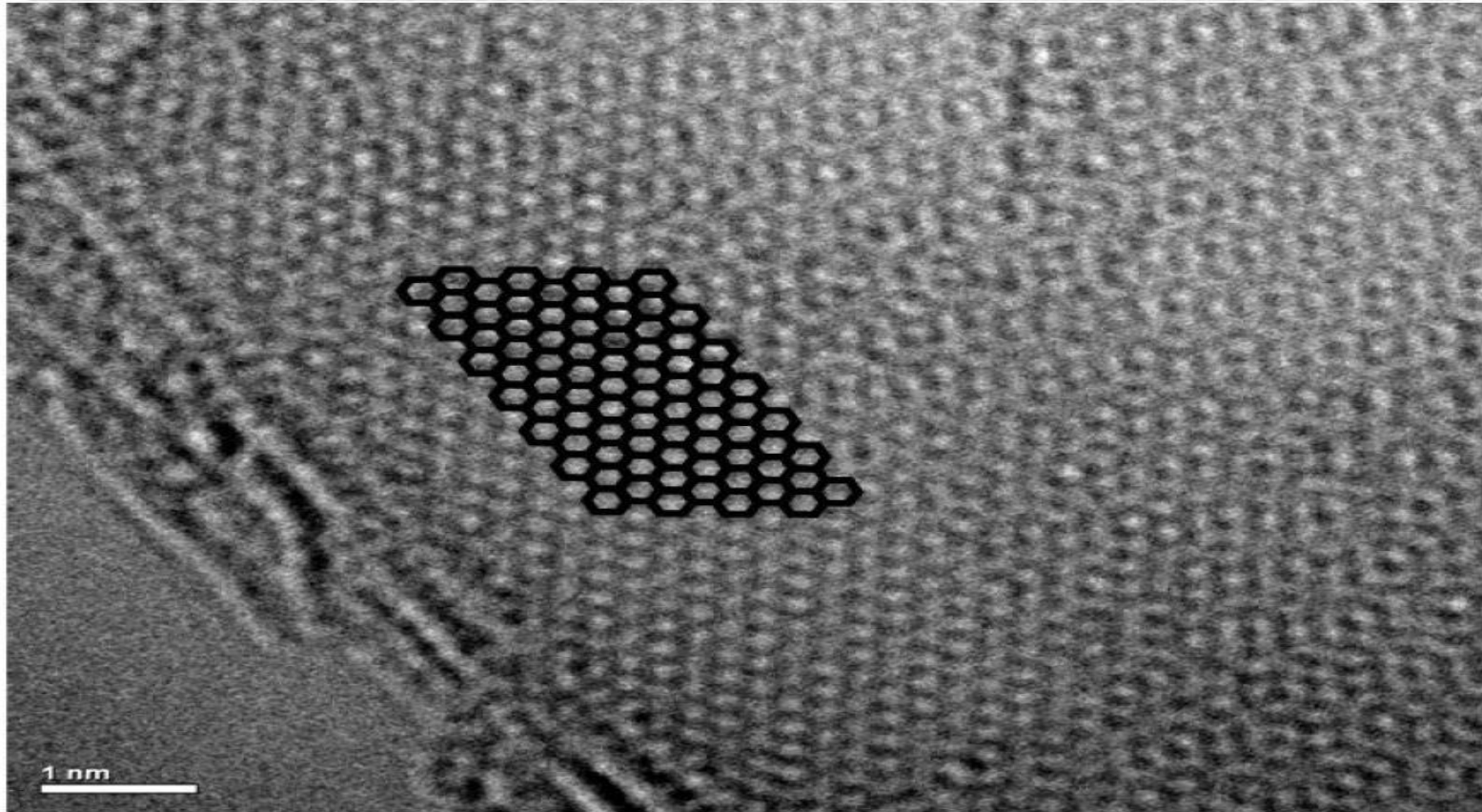
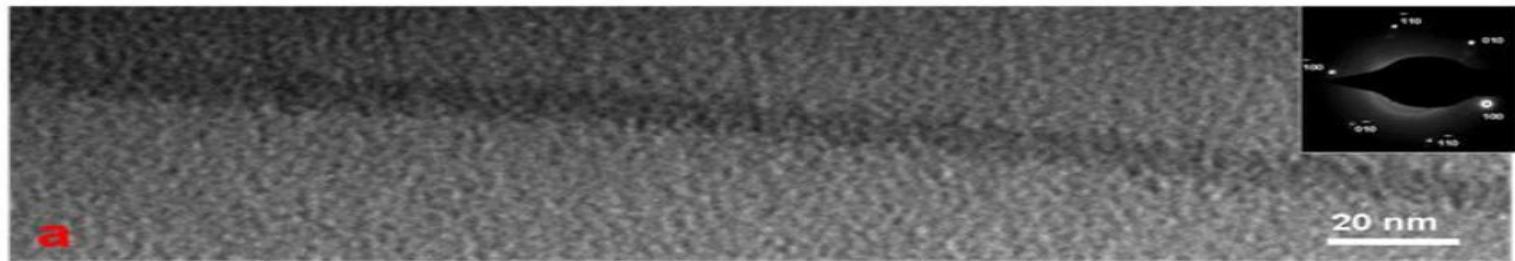
TEM and FESEM images



Bar sizes = (a) 250 nm, (b,g,l,j) 50 nm, (c,d) 500 nm, and (h) 1 μm .

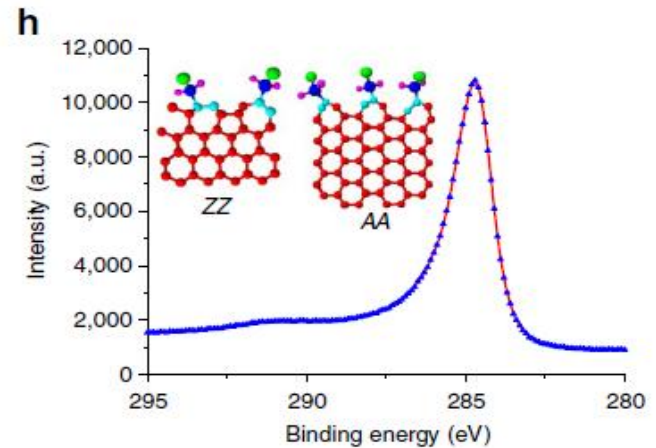
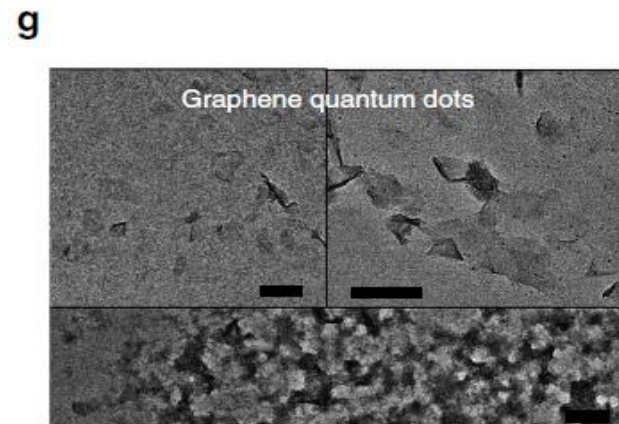
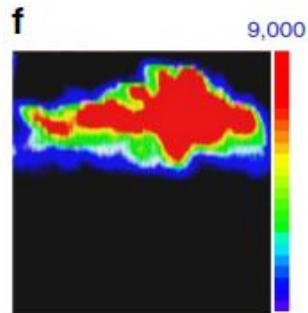
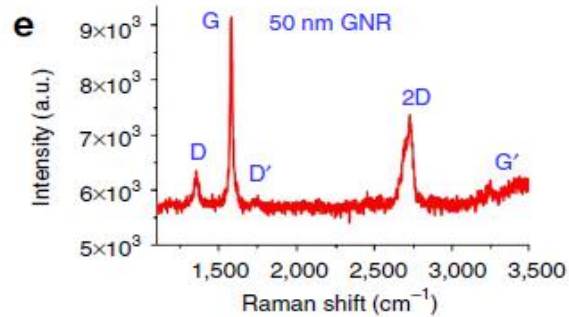
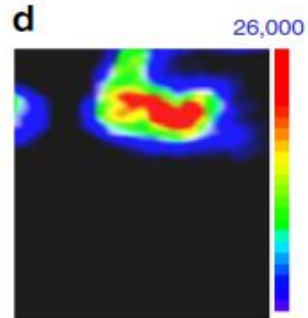
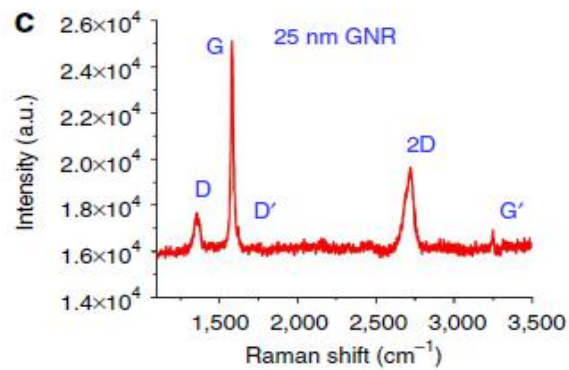
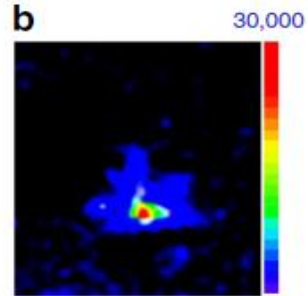
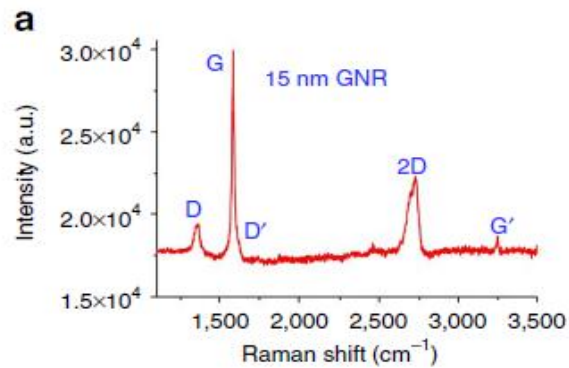


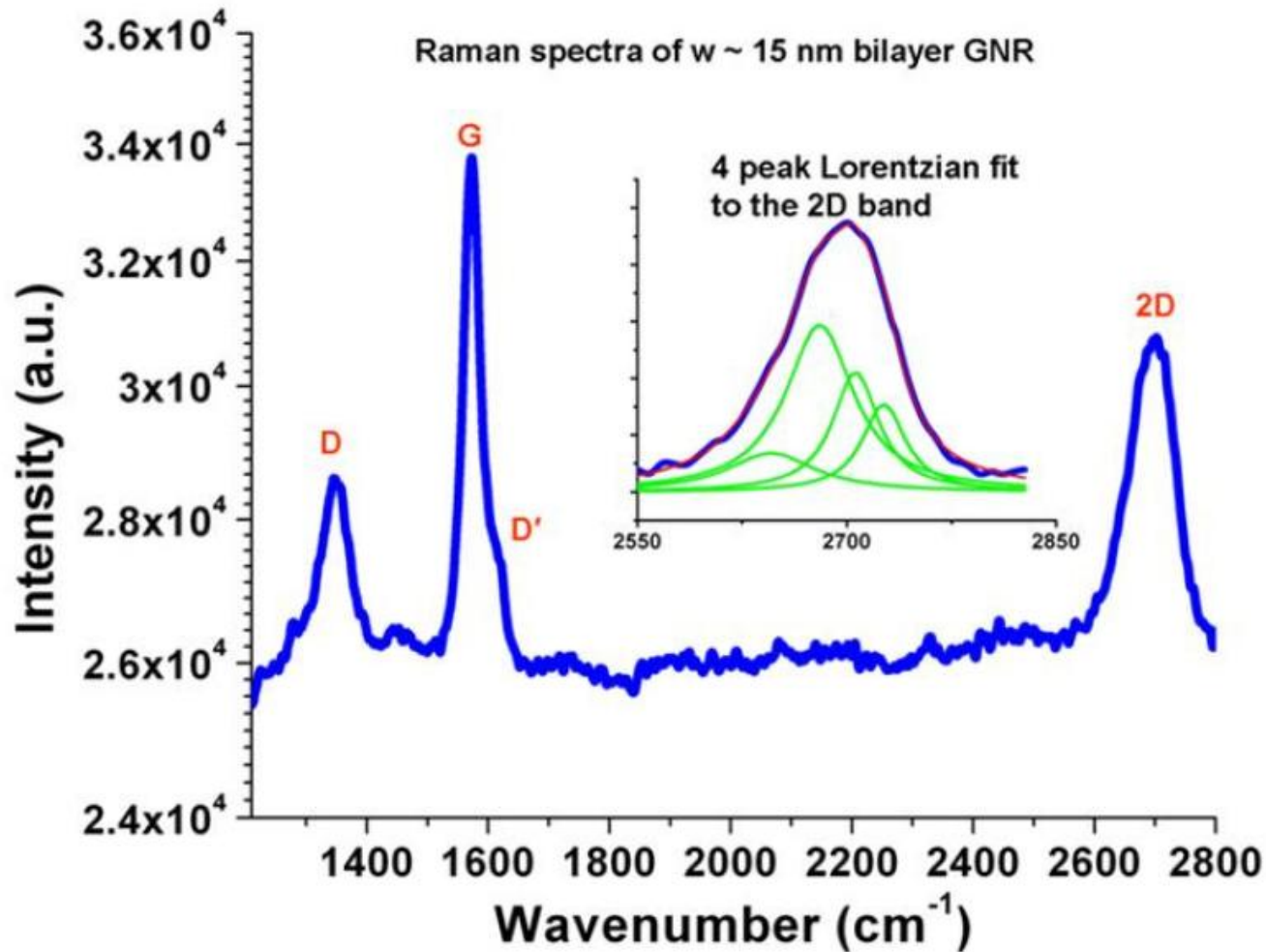
(a, b, c, d) TEM images of $w \sim 15, 25, 30$ and 40 nm GNRs. Inset of (a) is an FESEM images of $w \sim 5$ nm GNRs immobilized on silicon substrates.



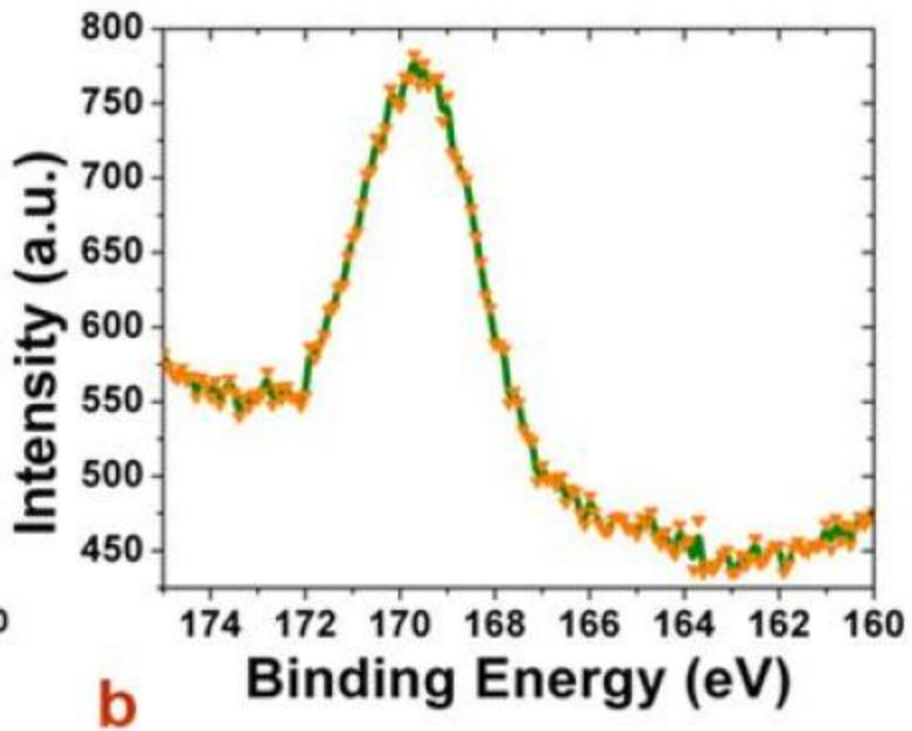
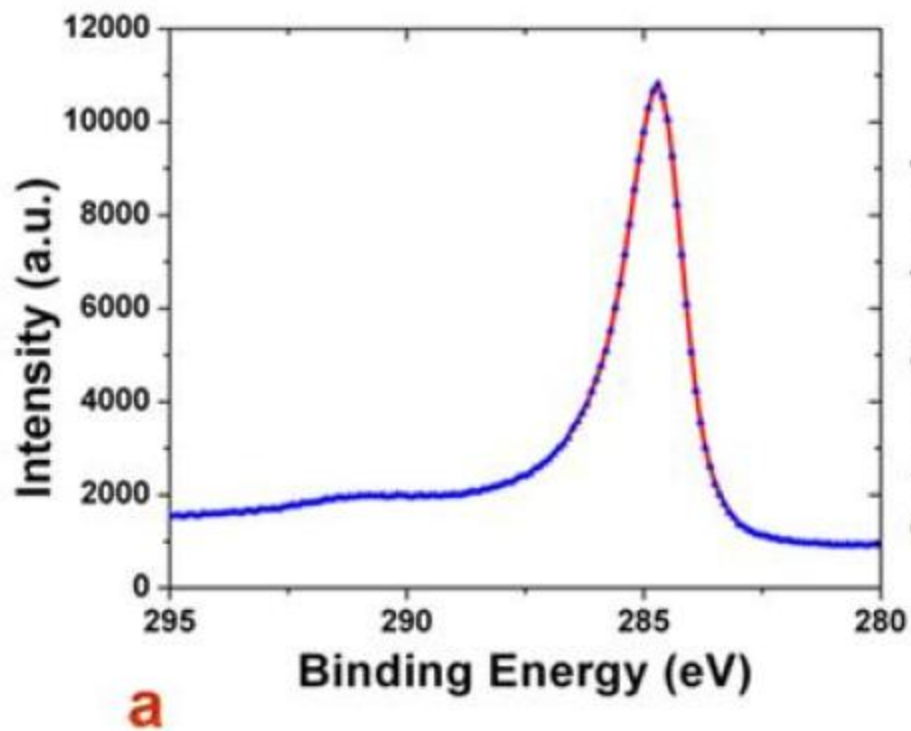
(a) HRTEM image of a $w \sim 15$ nm wide GNR showed width uniformity. A selected-area-electron-diffraction (SAED) pattern on the GNR shows a hexagonal pattern similar to that observed in graphene. (b) showing atomic lattice.

RAMAN and XPS

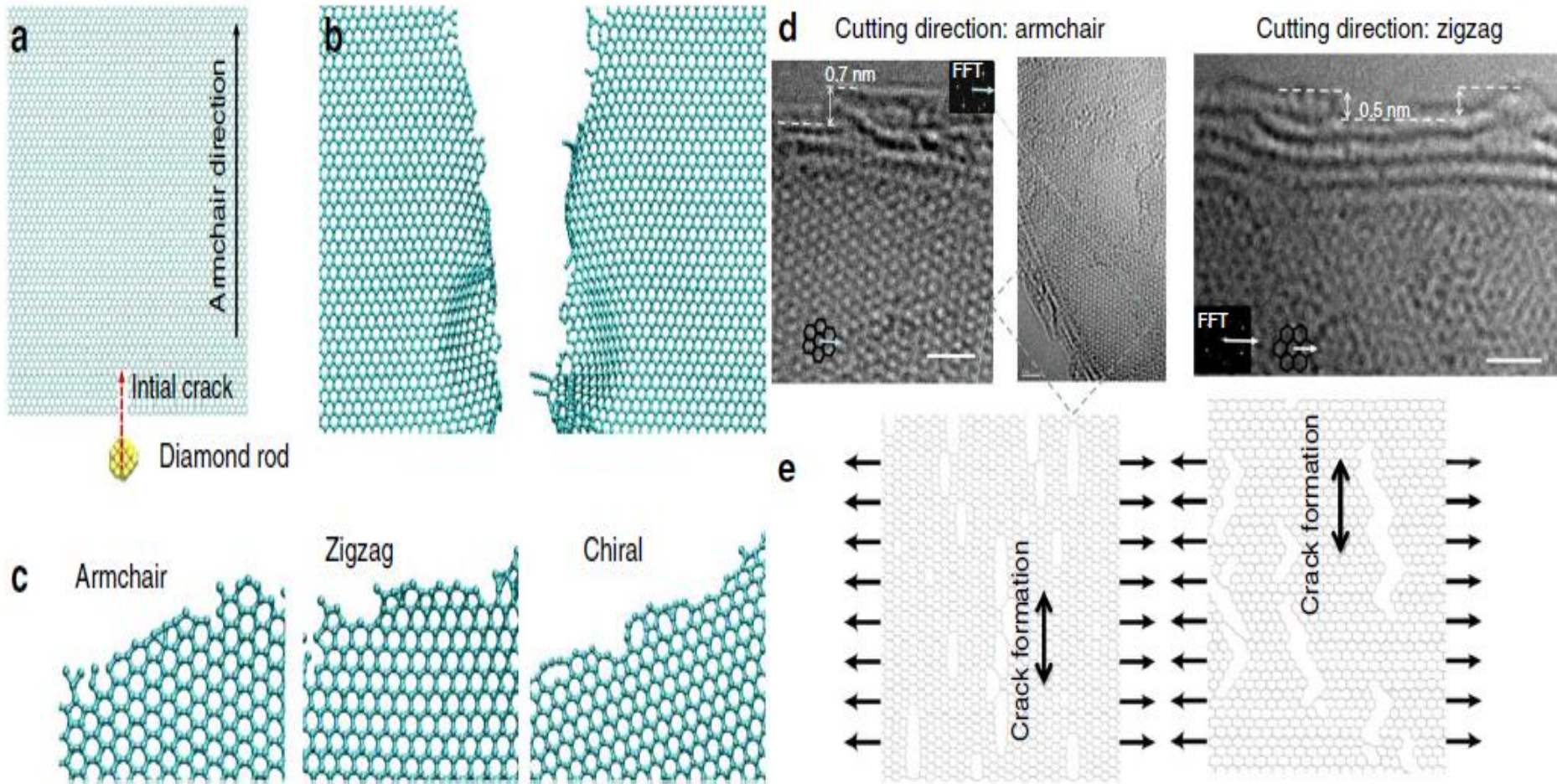


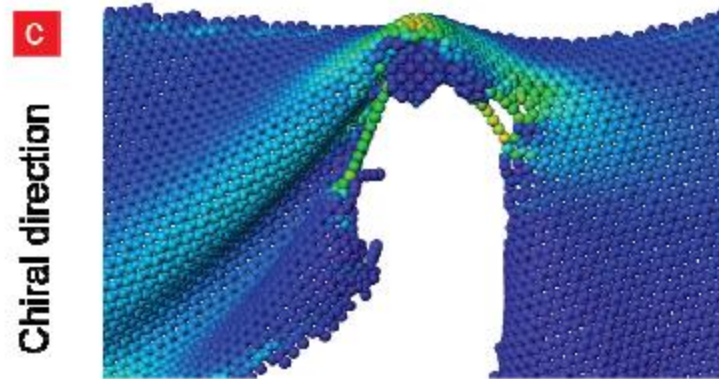
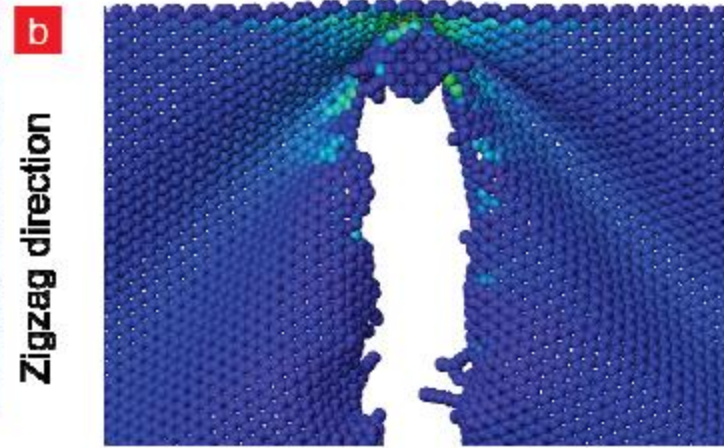
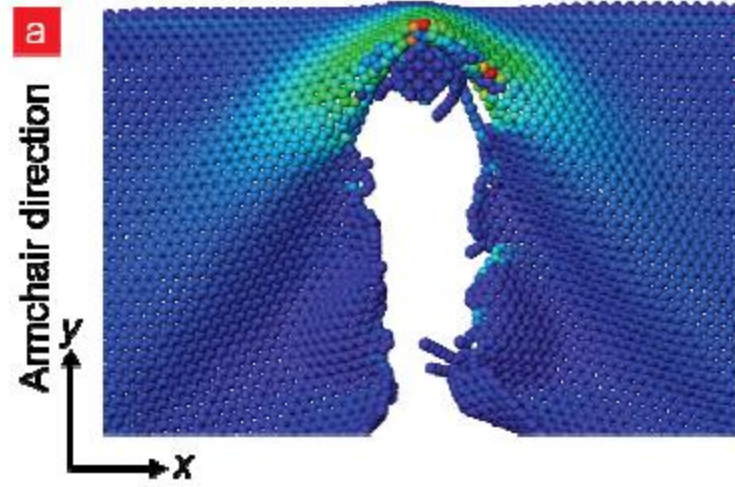


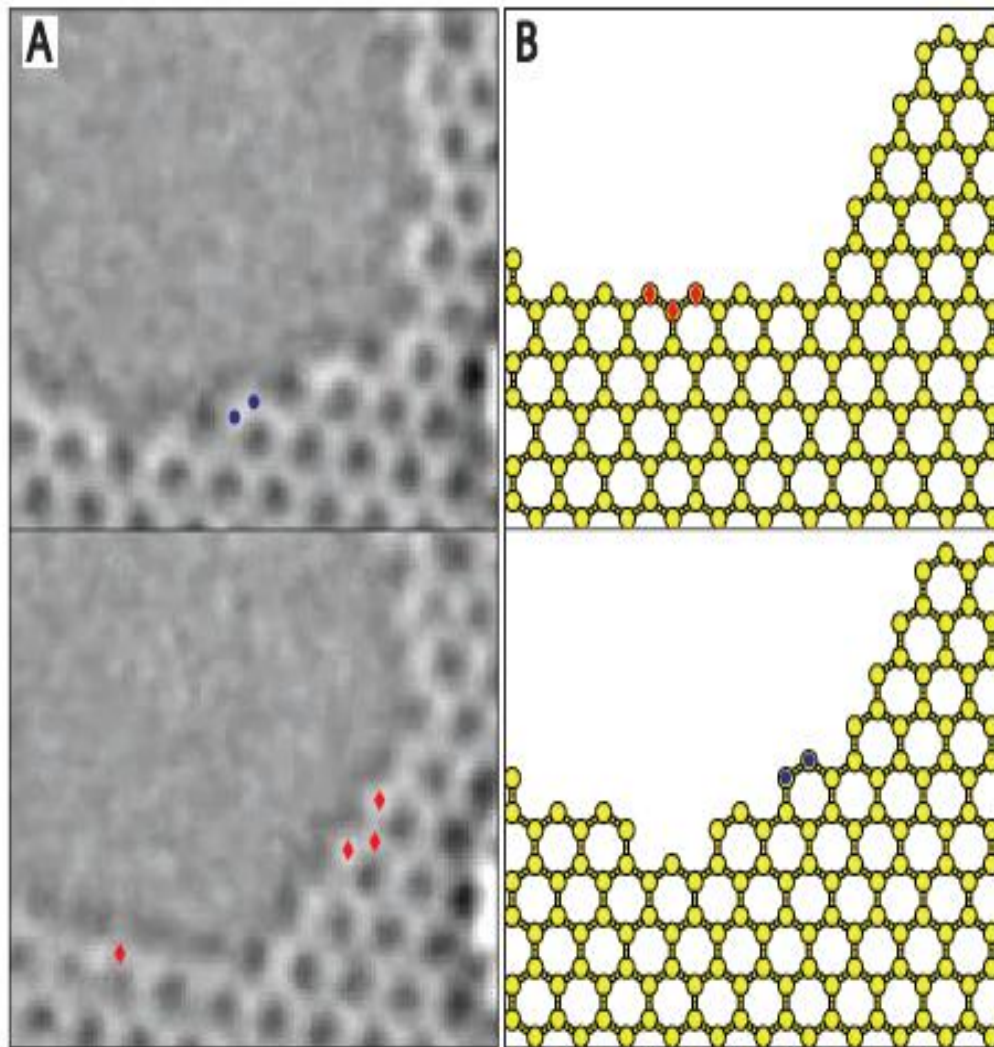
A typical conformal Raman mapping of a w ~ 15 nm wide GNR immobilized on a silicon dioxide surface. Inset of figure shows a successful 4 peak Lorentzian fit of the 2D band of the GNR attributing bilayer nature. The I_D/I_G was ~ 0.4-0.5



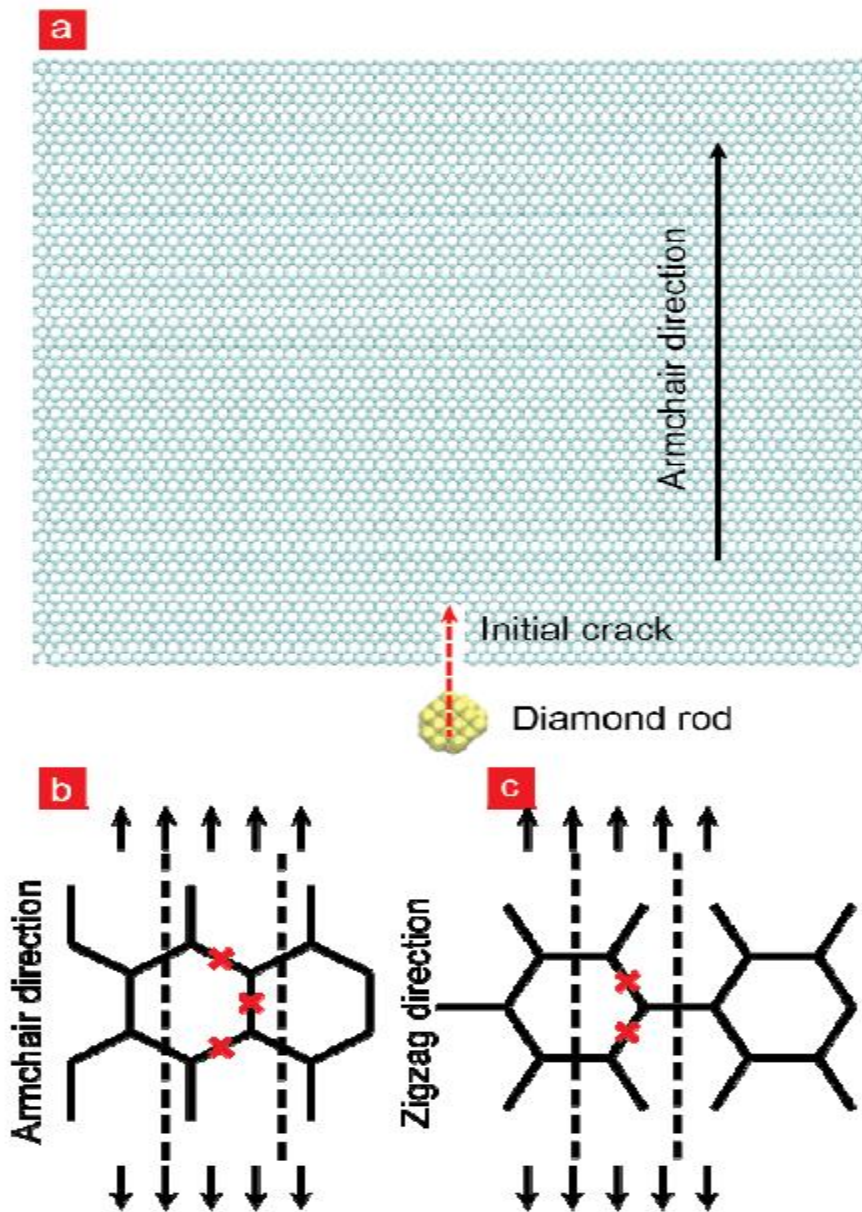
Molecular Dynamics simulations





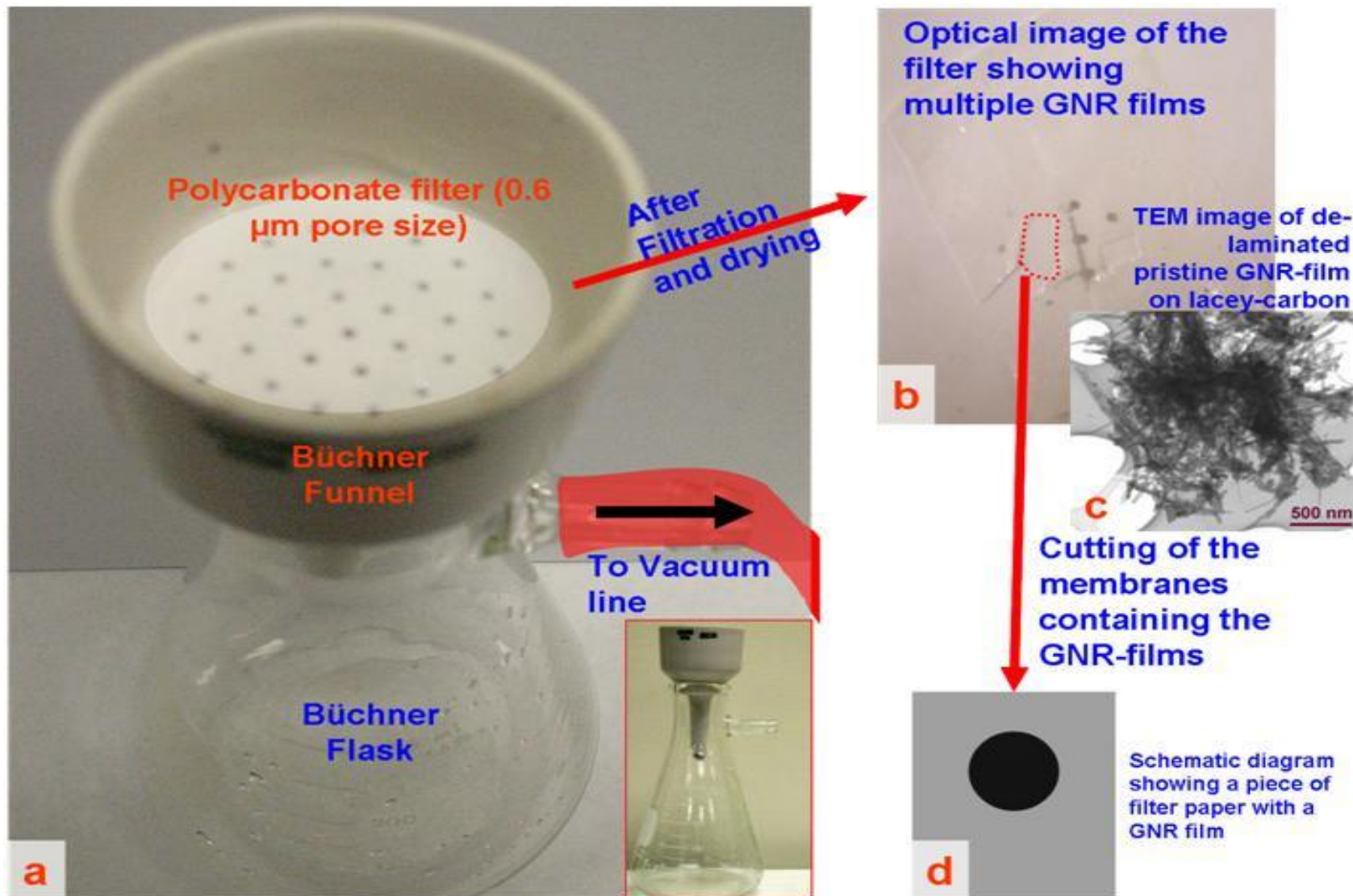


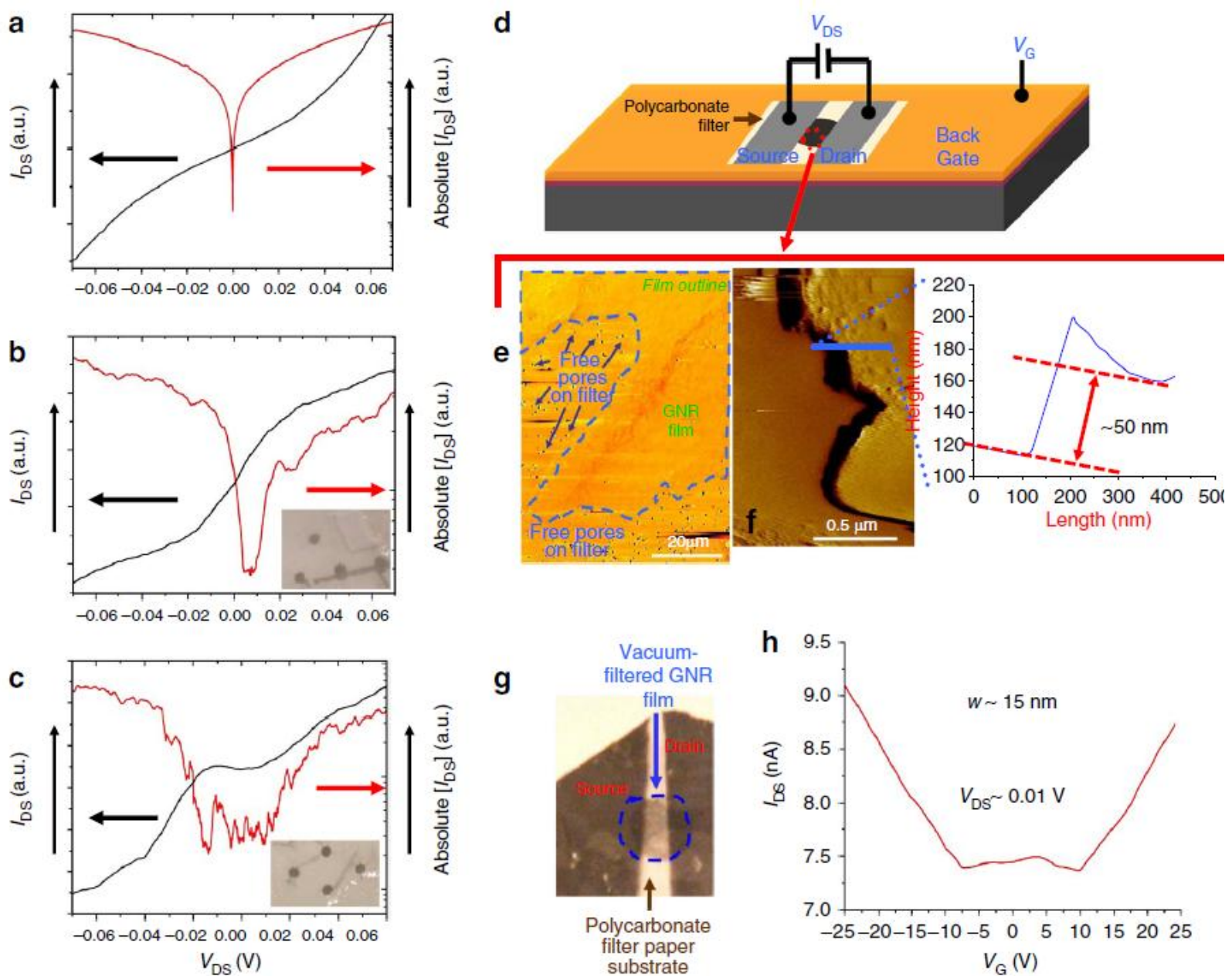
Edge reconfiguration. (A) Conversion of an armchair edge (top) to a zigzag edge (bottom) over the course of two frames, 14 and 15, taken at a 4-s interval. The two atoms marked as blue dots in the upper frame are gone in the lower frame, where four new carbon atoms are indicated as red diamonds. The 7-hexagon armchair edge is transformed into a 9-hexagon zigzag edge with a 60° turn. The transformation occurs due to migration of atoms along the edge. (B) Similar behavior is observed in the kinetic Monte Carlo simulation of hole growth, where three zigzag atoms (red diamonds, top) from frame 235 disappear and two armchair atoms (blue dots, bottom) appear in frame 239. Both frames in (B) have been flipped vertically.



Molecular dynamics simulations of the cutting process. a) shows the simulation setup of a graphene sheet with an initial crack and a diamond rod as the knife. b and c illustrate carbon-carbon bonds in the graphitic lattice that bear maximum loads under tensile loads from a static mechanics analysis. The distribution of these bonds defines the breaking pattern as shown perviously

Electrical characterization





Width of a GNR governs its bandgap ($\propto 1/w$), thin films of GNRs must exhibit width-dependent bandgap.

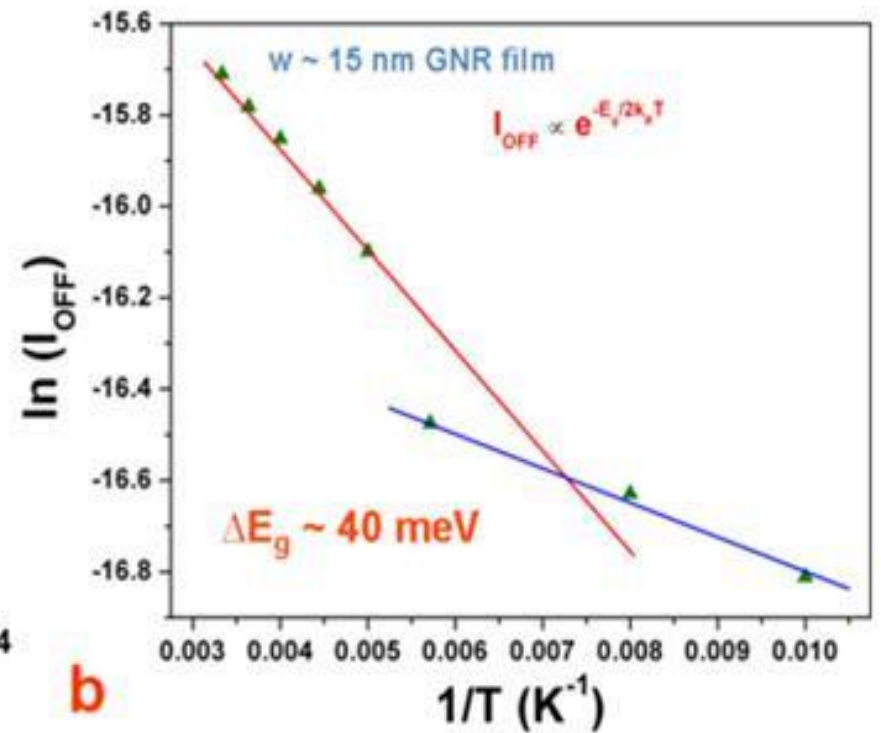
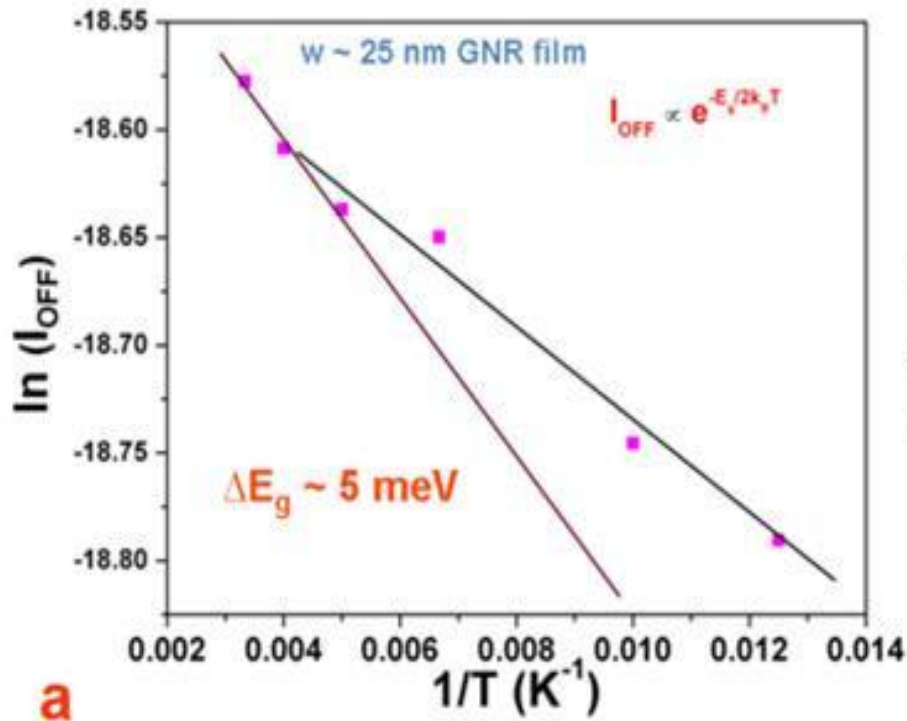
Electrical characterization of thin GNR-films.

(a,b,c) black line - show nonlinear transport behaviour.

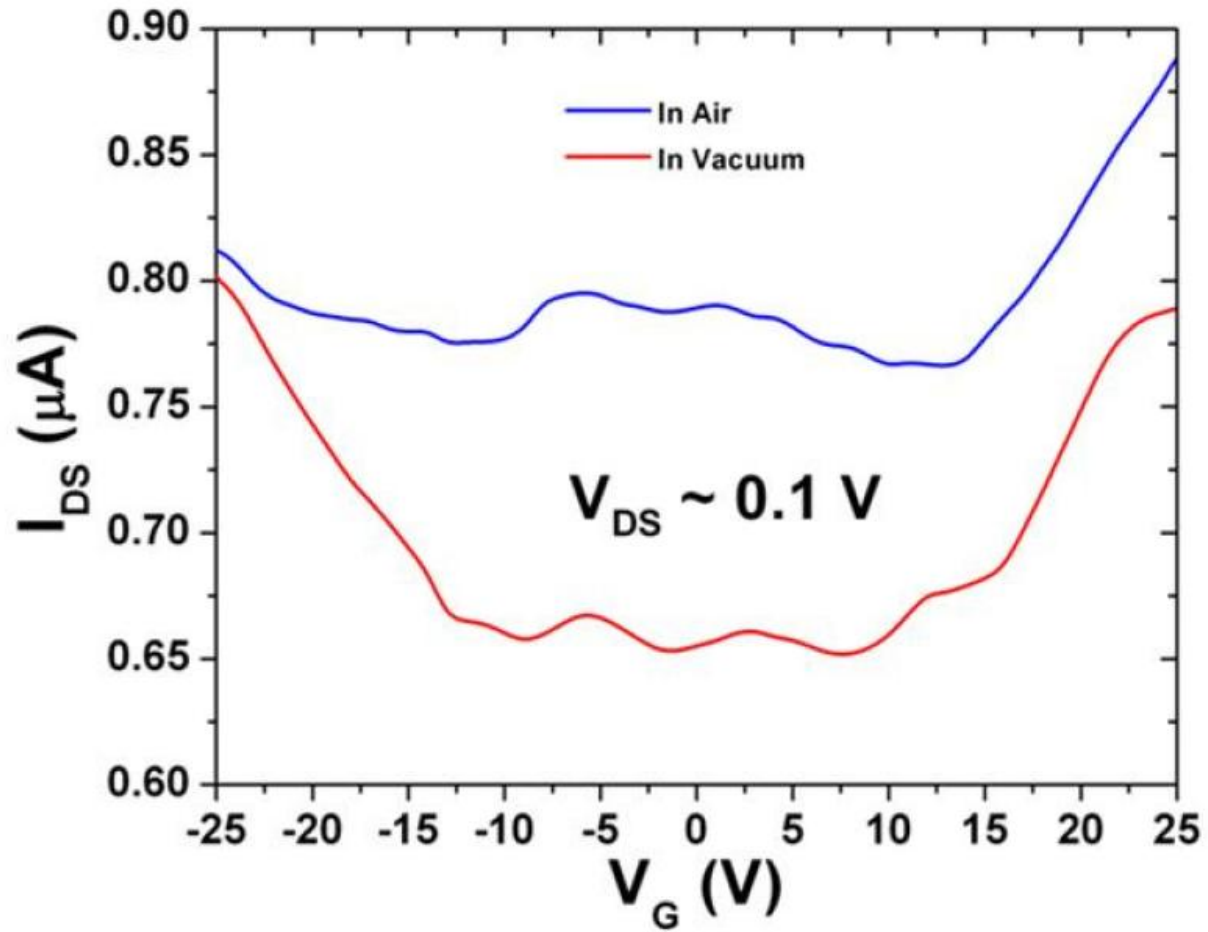
The edges of the bandgap were determined from the sharp current increase in the log-scale curve (red). Owing to the relatively large channel lengths of the GNR film-devices, the channel-length dependence of the nonlinear transport gap is expected to be negligible. A bandgap scaling with GNR width was observed: the bandgaps for the as-produced films with $w=50$, 25 and 15 nm GNRs were ~ 0 meV, ~ 10 meV and ~ 35 meV, respectively (this is appropriate because panel h shows that the conductivity is well centred around zero volt bias. After deposition of electrodes, these polycarbonate sheets were deposited on gold substrates as shown in panel d.

(f) Tapping-mode AFM(left inset) image of the GNR film shows a typical thickness of ~ 50 nm (right inset).

(h) A 15-nm GNR film at 10 mV (VDS), gated with voltage in the ± 25 V range exhibits a semiconducting behaviour with symmetric hole and electron densities. The electron mobility measured from transconductance is $\sim 20 \text{ cm}^2 \text{ V}^{-1} \text{ s}^{-1}$.



Typical temperature dependent transfer characteristics of the GNR-films



Summary and conclusion

- GNs were synthesized, via a versatile nanotomy process, with high structural control (shapes: squares, rectangles, ribbons and triangles; and size: adjusted at 5 nm resolution) and colloidal monodispersivity.
- The GNs are exfoliated from GNBs produced via nanotomy of HOPG. This highly versatile process can produce a variety of GN structures.
- Raman and the HRTEM measurement show that the GNs had relatively smooth edges;
- The MD simulations and HRTEM micrographs show that the edges are predominantly zigzag.
- Electrical studies show evolution of bandgap of thin GN films with GNR's width.

Thank you